IAF-92-0016
Time-Free Transfers Between Libration-Point Orbits in the Elliptic Restricted Problem

K. C. Howell and L. A. Hiday

School of Aeronautics and Astronautics
Purdue University
West Lafayette, Indiana
Tel. (317) 494-5786, Telex 276147, Fax (317) 494-0307

43rd CONGRESS OF THE INTERNATIONAL ASTRONAUTICAL FEDERATION

August 28-September 5, 1992/Washington, DC

TIME-FREE TRANSFERS BETWEEN LIBRATION-POINT ORBITS IN THE ELLIPTIC RESTRICTED PROBLEM

K. C. Howell* and L. A. Hiday**
Purdue University
West Lafayette, Indiana

Abstract

This work is part of a larger research effort directed toward the formulation of a strategy to design optimal time-free impulsive transfers between three-dimensional libration-point orbits in the vicinity of the interior L_1 libration point of the Sun-Earth/Moon barycenter system. Inferior transfers that move a spacecraft from a large halo orbit to a smaller halo orbit are considered here. Primer vector theory is applied to non-optimal impulsive trajectories in the elliptic restricted three-body problem in order to establish whether the implementation of a coast in the initial orbit, a coast in the final orbit, or dual coasts accomplishes a reduction in fuel expenditure. The addition of interior impulses is also considered. Results indicate that a substantial savings in fuel can be achieved by the allowance for coastal periods on the specified libration-point orbits. The resulting time-free inferior transfers are compared to time-free superior transfers between halo orbits of equal z-amplitude separation.

I. Introduction

Associated with the general problem of minimum-fuel trajectories in an inverse square gravitational field is a well-developed theory stemming, in great part, from Lawden's pioneering work.[1] Lawden establishes the necessary conditions that must be satisfied by the *primer vector* (i.e., the vector comprised of the adjoint variables associated with the velocity) and its derivative on an impulsive trajectory that is considered optimal. The addition of an interior impulse, which renders the time of flight on the transfer unchanged, as well as the implementation of coasts in the initial and final orbits, which results in an altered transfer time of flight, have been examined as means of improving the performance of a non-optimal reference solution. Numerous researchers have employed these techniques to obtain minimum-fuel trajectories in the two-body problem.

In contrast, the design of transfers between two orbits in the three-body problem has remained relatively unexplored. Two previous independent investigations are known that examine transfers between halo or halo-type orbits, and these studies are distinguished by the method of solution and by the *inferior* (large halo → small halo) or *superior* (small halo → large halo) nature of the transfer. First, Pernicka[2] briefly examines superior transfers between two nearly periodic halo orbits about a collinear libration point in the elliptic restricted three-body problem. The investigation utilizes a trial-and-error method to determine a path that approximately connects the specified departure and arrival locations. The optimality of the resultant two-impulse transfer is not explored. Secondly, Gómez *et al.*[3] use manifold theory to study an inferior transfer between halo orbits about a collinear libration point in the circular restricted three-body problem. More recently, primer vector theory has been extended to the elliptic restricted three-body problem by the authors and applied to time-fixed[4] and time-free[5] superior transfers between libration-point orbits.

This study investigates the time-free optimization of inferior transfers between halo orbits near the L_1 libration point in the elliptic restricted three-body problem. The inclusion of either an initial or final coast on a reference solution produces a *time-free* transfer trajectory. (For clarity, note that the solution might also be discussed as a time-fixed transfer between specified endpoints that includes the option of initial and final coasts.) The work contained herein augments the research presented in Reference 5 that examines the optimization of time-free superior transfers using primer vector theory. First a new method for the construction of a nominal trajectory is outlined. Then, the optimization process developed in Reference 5 is applied to the nominal or reference solution. Here, optimum is defined to be minimum characteristic velocity or, equivalently, minimum sum of the magnitudes of the impulsive maneuvers. The solution for the optimal times of departure from the initial halo orbit and arrival in the final orbit are obtained using a multivariable search procedure. Since such methods essentially employ a gradient technique, the solution for the transfer converges only to a minimum within the same "valley" as the nominal solution. Hence, the approach outlined here results in a locally optimal transfer trajectory, and other solutions may exist.

Once the best two-impulse time-free transfer is obtained, the optimality of this solution is examined, and the necessity of an additional impulse to reduce total fuel expenditure is ascertained utilizing a strategy previously developed.[4] In order to investigate the effect

* Associate Professor, School of Aeronautics and Astronautics.
**Graduate Student, School of Aeronautics and Astronautics.

of declivity and acclivity on the cost of a transfer trajectory between two libration-point orbits, the correlation between the superior time-free transfers presented in Reference 5 and the inferior transfers constructed here is explored.

II. Force Model and the Initial and Final Orbits

The model representing the actual forces acting on the spacecraft is chosen to be the elliptic restricted three-body model for the Sun-Earth/Moon barycenter system (i.e., Earth and Moon are considered a single body of mass equal to the sum of their individual masses placed at their barycenter). The initial and final libration-point orbits are selected to be halo orbits. In the most basic sense, halo orbits are three-dimensional trajectories that are periodic relative to the usual coordinate frame associated with the restricted problem. Upon specification of an injection date, the halo orbits are approximated using Richardson's[6] third order analytic approximation. The approximation for each halo provides the requisite initial estimate for the two-level iteration scheme at the core of the numerical integration technique developed by Howell and Pernicka.[7] The resulting integrated halo trajectories are not exactly periodic; thus, they are not true halos as originally defined. However, they render very close approximations, and the label 'halo orbit' usually includes such variations. An example of such a numerically determined 'near-halo' is shown in Figure 1. The orbit is located in the vicinity of the interior L_1 libration point in the Sun-Earth/Moon system. Three projections of the orbit are shown, with the origin in each plot corresponding to the oscillating L_1 point. The three axes associated with the figure are defined consistent with the rotating frame typically used with the restricted three-body problem. Suppose then that a transfer is desired that moves a spacecraft from an initial halo orbit A, having an out-of-plane z-amplitude A_{z_A} (as shown in Figure 1), to a final halo orbit B, having a z-amplitude A_{z_B}. In general, A_{z_B} may be larger or smaller than A_{z_A}. Once the initial and final halo orbits are numerically determined, the departure and arrival locations on the halo orbits are arbitrarily selected so that $\bar{x}_A$, the position vector at departure from orbit A, and $\bar{x}_B$, the position vector at arrival at orbit B, are specified.

III. Construction of a Nominal Transfer Trajectory

The transfer path connecting $\bar{x}_A$ to $\bar{x}_B$ is actually a portion of a more general Lissajous trajectory, and the construction of this transfer trajectory can be accomplished using only knowledge of the numerical solutions corresponding to the two halo orbits. This construction is essentially a three step process.

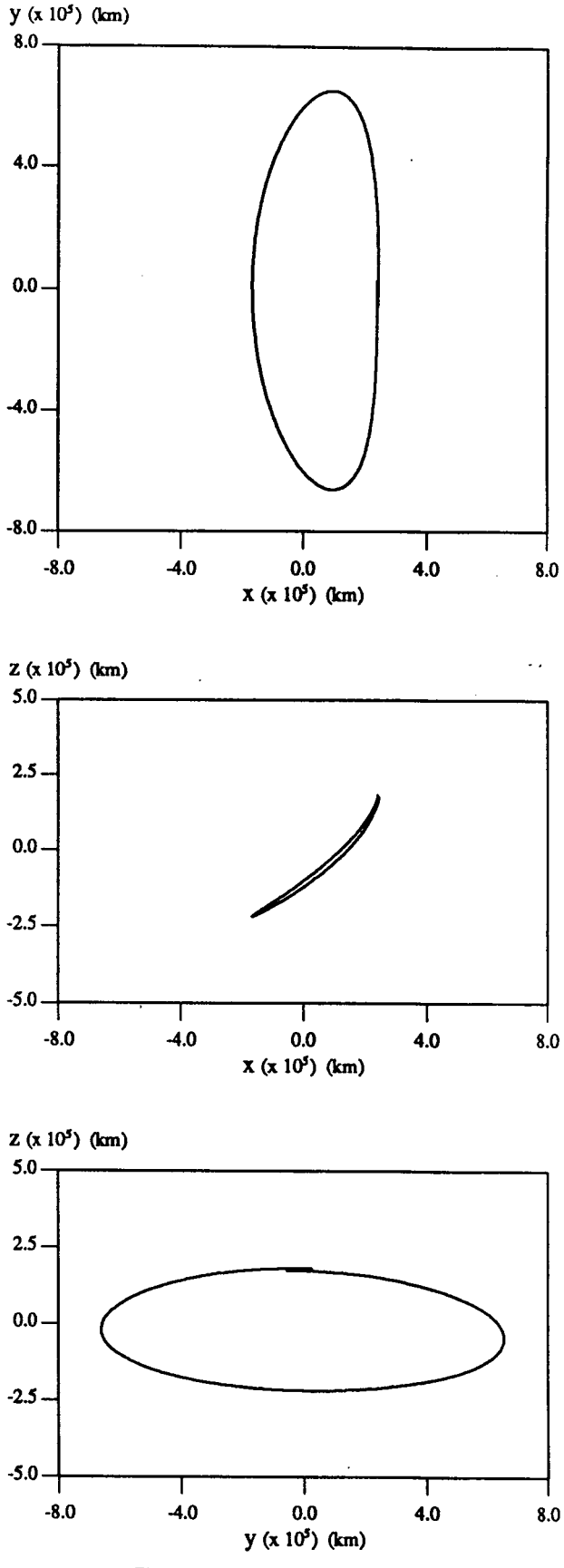

Fig. 1 Example of a 'Near-Halo' Orbit

A Spiral Method for Target Point Estimation

The transfer path construction process will employ the numerical algorithm, detailed in Reference 7, for determination of libration-point orbits. The algorithm assumes reasonably good approximations for a number of spacecraft position and velocity states at particular points (called *target points*) along the trajectory. Target points are typically spaced at quarter-rev or half-rev intervals. (One revolution about L_1 is defined in the y-z and/or x-y projection.) Initially, the integration algorithm determines a path, connecting the target points, that is continuous in position but may be discontinuous in velocity. The target points are then shifted in order to drive the velocity discontinuities to zero. Initial estimates for the target points and corresponding velocities on each trajectory segment that will comprise the complete path must be made available for input into the numerical integration algorithm. Estimates for the appropriate target point states along the initial and final segments are obtained from the numerical process that produces the halo orbits. A relatively straightforward method is then used to obtain estimates on the transfer segment of the trajectory. Assuming that the integration routine implements a quarter-rev patching scheme and that a 1-rev transfer is to be constructed, only the three interior target points on the transfer must be approximated; whereas, the two target points that bound the transfer are simply taken to be the departure and arrival positions and velocities on halo orbits A and B, respectively. The three interior target points are estimated using those target points on orbits A and B which occur near the points of minimum and maximum y- and z-excursion.

For example, given a typical pair of libration-point orbits, the trajectories might proceed in counter-clockwise directions when viewed in a y-z projection. As a portion of a Lissajous path, a 1-rev transfer will appear similarly. If departure from the initial halo occurs near the maximum z-excursion point of orbit A, the first interior target point that must be estimated on the transfer trajectory is located near the minimum y-excursion points of the halo orbits. The second and third interior target points would then lie near the minimum z-excursions and near the maximum y-excursions of the halo orbits, respectively. Experience with superior transfers[5] suggests that good estimates for these target points and their corresponding velocities can be obtained from weighted averages of the positions and velocities on orbits A and B. For the first interior target point, the position and velocity at the minimum y-excursion on orbit A are weighted three times more than those on orbit B. For the second interior target point, the minimum z-excursions and corresponding velocities on the two halo orbits are weighted equally; additionally, the position and velocity at the maximum y-excursion on orbit B are weighted three times more than those on orbit A for the third and final interior target point. This method of constructing estimates for the position and velocity at quarter-rev intervals on the transfer trajectory essentially creates a *spiral* of target points from orbit A to orbit B. (Note that this process differs from that used to obtain nominal superior transfers.[5])

With the target points on the transfer approximated and with those on the halo orbits specified from numerical results, the entire trajectory (orbit A, transfer trajectory, orbit B) is input to a suitable trajectory determination algorithm[7] to produce a numerical solution that is continuous in position; moreover, since no $\Delta\bar{v}$ maneuvers are imposed at the departure and arrival locations on the halo orbits, the trajectory is continuous in velocity as well. However, due to the nature of the corrections process that shifts the target points to eliminate velocity discontinuities, the omission of these impulsive velocity maneuvers results in a solution that diverges from the halo orbits, for no transfer trajectory can be constructed that moves precisely between orbits A and B without the expenditure of fuel. Consequently, $\Delta\bar{v}$ maneuvers must be inserted to construct a solution that passes through the desired departure and arrival positions. The problem has thus been redefined as follows: Given a numerical solution in the elliptic restricted problem, a neighboring solution is sought (including two $\Delta\bar{v}$ maneuvers) such that the path (i) is initially constrained to match orbit A to the specified departure point; (ii) passes through the transfer; and, (iii) subsequent to the specified arrival point, is constrained to match orbit B.

A Differential Corrections Procedure

Let a quantity be designated with a *tilde* if its *desired* value on the halo orbits is known. So, from the individual numerical integrations of halo orbits A and B, the quantities $\tilde{\bar{x}}_A$, $\tilde{\bar{v}}_A$ and $\tilde{\bar{x}}_B$, $\tilde{\bar{v}}_B$ denote the position and velocity at departure from orbit A and at arrival at orbit B, respectively. For a given numerically determined reference solution for the entire trajectory, assume that the impulsive maneuver $\Delta\bar{v}_0$ is implemented at departure from orbit A, which is located on the transfer trajectory at the point $\bar{x}_0$ at $t = t_0$. (Note that $\Delta\bar{v}_0 = 0$ on the initial reference solution, but $\bar{x}_0$ does not equal the desired position $\tilde{\bar{x}}_A$.) If the velocity on reference orbit A at $t = t_{0^-}$ is denoted by $\bar{v}_A$, then the velocity on the transfer at $t = t_{0^+}$, denoted by $\bar{v}_0$, can be expressed as

$$\bar{v}_0 = \bar{v}_A + \Delta\bar{v}_0 \,. \qquad (1)$$

Let a quantity on an *improved*, or *differentially corrected*, trajectory be denoted with a *prime*. So, the contemporaneous variation in velocity after departure is

$$\delta\bar{v}_{0^+} = \bar{v}_0' - \bar{v}_0 \,. \qquad (2)$$

Evaluating equation (1) on the improved trajectory and

substituting the resultant expression as well as equation (1) into (2),

$$\delta\bar{v}_{0^+} = (\bar{v}_A' + \Delta\bar{v}_0') - (\bar{v}_A + \Delta\bar{v}_0) . \quad (3)$$

Rearranging equation (3),

$$\Delta\bar{v}_0' = \delta\bar{v}_{0^+} + (\bar{v}_A - \tilde{\bar{v}}_A) + \Delta\bar{v}_0 , \quad (4)$$

where a $\bar{v}_A'$ is replaced by $\tilde{\bar{v}}_A$ because the desired value of this quantity on the differentially corrected solution is known. Thus, equation (4) provides an expression for the improved initial impulsive maneuver in terms of the unknown $\delta\bar{v}_{0^+}$, the specified difference in the reference and desired velocities on orbit A, and the reference initial impulsive maneuver. The only unknown quantity on the right side of (4) is $\delta\bar{v}_{0^+}$, the computation of which will be addressed shortly.

Next, however, consider impulsive maneuver $\Delta\bar{v}_f$ executed upon arrival at orbit B and located on the transfer trajectory at the point $\bar{x}_f$ at $t = t_f$. (Note that $\Delta\bar{v}_f = 0$ on the initial reference solution, but $\bar{x}_f$ does not initially equal the desired position $\tilde{\bar{x}}_B$). The final impulsive maneuver on the differentially corrected solution is represented as

$$\Delta\bar{v}_f' = \tilde{\bar{v}}_B - \bar{v}_f' , \quad (5)$$

where, again, the symbol $\tilde{\bar{v}}_B$ is employed to stress that the desired value of the velocity on orbit B is known; additionally, $\bar{v}_f'$ can be expressed in terms of the contemporaneous variation in velocity at $t = t_f^-$ as

$$\bar{v}_f' = \bar{v}_f + \delta\bar{v}_{f^-} . \quad (6)$$

In a form analogous to equation (4) or from substitution of equation (6) into (5),

$$\Delta\bar{v}_f' = (\tilde{\bar{v}}_B - \bar{v}_B) - \delta\bar{v}_{f^-} + \Delta\bar{v}_f = \tilde{\bar{v}}_B - \bar{v}_f - \delta\bar{v}_{f^-} , \quad (7)$$

where the second form of (7) is used since the value of $\tilde{\bar{v}}_B$ and the reference value of $\bar{v}_f$ are known quantities; however, the computation of $\delta\bar{v}_{f^-}$ remains to be addressed.

In order to evaluate equations (4) and (7), the contemporaneous variations in velocity subsequent to departure from orbit A and prior to arrival at orbit B must be determined. These two quantities can be computed utilizing the state transition matrix evaluated on the transfer arc $t_0 \le t \le t_f$ to yield

$$\begin{bmatrix} \delta\bar{x}_f \\ \delta\bar{v}_{f^-} \end{bmatrix} = \begin{bmatrix} \phi_{11}(t_f,t_0) & \phi_{12}(t_f,t_0) \\ \phi_{21}(t_f,t_0) & \phi_{22}(t_f,t_0) \end{bmatrix} \begin{bmatrix} \delta\bar{x}_0 \\ \delta\bar{v}_{0^+} \end{bmatrix} . \quad (8)$$

The quantities $\delta\bar{x}_0$ and $\delta\bar{x}_f$, which simply represent the differences between the desired locations of the impulsive maneuvers and those determined from the numerically integrated reference solution for the entire trajectory, can be expressed as

$$\delta\bar{x}_0 = \tilde{\bar{x}}_A - \bar{x}_0 \quad (9a)$$

$$\delta\bar{x}_f = \tilde{\bar{x}}_B - \bar{x}_f . \quad (9b)$$

Equations (8) can be rearranged to yield

$$\delta\bar{v}_{0^+} = \phi_{12}^{-1}(t_f,t_0)\left[\delta\bar{x}_f - \phi_{11}(t_f,t_0)\delta\bar{x}_0\right] . \quad (10a)$$

$$\delta\bar{v}_{f^-} = \phi_{21}(t_f,t_0)\delta\bar{x}_0 + \phi_{22}(t_f,t_0)\delta\bar{v}_{0^+} , \quad (10b)$$

and substituting equation (10a) into (10b) renders

$$\delta\bar{v}_{f^-} = \phi_{21}(t_f,t_0)\delta\bar{x}_0 + \phi_{22}(t_f,t_0)\phi_{12}^{-1}(t_f,t_0) \left[\delta\bar{x}_f - \phi_{11}(t_f,t_0)\delta\bar{x}_0\right] . \quad (11)$$

Finally, with expressions (10a) and (11) for the contemporaneous variation in velocity subsequent to and prior to the impulsive maneuvers, respectively, the differentially corrected $\Delta\bar{v}$'s can now be computed. Substituting (10a) into equation (4) yields

$$\Delta\bar{v}_0' = \phi_{12}^{-1}(t_f,t_0)\left[\delta\bar{x}_f - \phi_{11}(t_f,t_0)\delta\bar{x}_0\right] + (\bar{v}_A - \tilde{\bar{v}}_A) + \Delta\bar{v}_0 , \quad (12)$$

and substituting (11) into equation (7) yields

$$\Delta\bar{v}_f' = \phi_{22}(t_f,t_0)\phi_{12}^{-1}(t_f,t_0)\left[\phi_{11}(t_f,t_0)\delta\bar{x}_0 - \delta\bar{x}_f\right] - \phi_{21}(t_f,t_0)\delta\bar{x}_0 + \tilde{\bar{v}}_B - \bar{v}_f . \quad (13)$$

Consequently, the impulsive maneuvers on the numerically determined reference trajectory should be differentially corrected to the values computed in equations (12) and (13), where $\delta\bar{x}_0$ and $\delta\bar{x}_f$ are computed from (9), such that the improved trajectory more closely approximates the desired locations of departure and arrival on the halo orbits. Computation of differentially corrected trajectories continues iteratively until the departure and arrival positions on the improved path lie within a selected tolerance region. Provided that the difference in z-amplitudes of the two halo orbits is fairly small, convergence to the desired positions is achieved. The primary benefit of this differential corrections routine is the refined estimation of the targets points on the transfer trajectory that connects halo orbits A and B.

Although the differential corrections procedure outlined above produces a complete solution that converges to the departure and arrival locations on the respective halo orbits A and B, the other points on the halo orbit segments of the integrated trajectory may diverge from those position coordinates desired on the halo orbits. That is, the differential corrections algorithm only ensures convergence to the last point on orbit A and to the first point on orbit B; all other points representing the portions of the integrated trajectory that correspond to the initial and final halo orbits may remain far removed from the associated coordinates on the

specified halos. Therefore, the components of the impulsive maneuvers must be further modified to accomplish convergence of the halo orbit segments of the complete integrated trajectory to the desired orbits A and B. This modification is currently performed manually using a visual comparison of the integrated solution to the desired halo orbits in order to repeatedly adjust the $\Delta\bar{v}$ maneuvers. Despite the subjective nature of this procedure, insight into the appropriate alterations of the velocity components is readily gained, and nominal transfers between two libration-point orbits can be constructed in a straightforward and rapid fashion.

A Continuation Algorithm

Not surprisingly, if the difference in the z-amplitudes of halo orbits A and B becomes too great, the differential corrections routine will fail to converge to the desired coordinates of departure and arrival. Hence, the original formulation of the single-path determination of a nominal transfer from halo orbit A to halo orbit B must be recast as the construction of multiple nominal transfers from halo orbit A to a series of intermediate halo orbits that culminates at halo orbit B. Note that the intermediate nominal transfers are not arranged consecutively; rather, each nominal contributes to the construction of the successive transfer such that the outcome of the algorithm is still a 1-rev transfer trajectory. Introduce an intermediate halo orbit C that has a z-amplitude $A_{z_C} = A_{z_A} + \Delta A_z$, where ΔA_z is chosen at the discretion of the trajectory designer. A transfer trajectory passing through the specified points of departure on orbit A and arrival on orbit C is then constructed utilizing the spiral method of target point estimation and the differential corrections procedure for determination of the impulsive maneuvers. The resultant complete trajectory (orbit A, transfer trajectory, orbit C) will not necessarily converge to the halo orbits over the appropriate segments; thus, the components of the impulsive maneuvers are modified manually until the complete numerical solution converges to the prescribed initial and final orbits. A nominal transfer between two halo orbits of z-amplitude A_{z_A} and A_{z_C} results.

However, the ultimate goal is the determination of a nominal transfer to the final halo orbit B possessing a z-amplitude of A_{z_B}. If the difference in z-amplitudes of orbits B and C is greater than the increment ΔA_z, continue the series of intermediate halo orbits with the introduction of another orbit D having z-amplitude A_{z_D} such that $A_{z_D} = A_{z_C} + \Delta A_z$. With the aid of the nominal transfer between orbits A and C, the procedure for construction of a nominal transfer from halo orbit A to halo orbit D is considerably abbreviated from that presented above. The target points on the nominal transfer between halo orbits A and C are taken as approximations to the corresponding target points on the transfer from orbit A to orbit D. Consequently, the spiral method of target point estimation is omitted from this step in the algorithm. Often the differential corrections procedure may be omitted as well, and only the manual modification of the impulsive maneuvers is required to produce the desired transfer.

The introduction of intermediate halo orbits and the subsequent construction of nominal transfers from orbit A to the intermediate halos continue until the difference in z-amplitude between the last intermediate halo and the final halo orbit B is less than ΔA_z. Values of ΔA_z on the order of 10,000 km to 50,000 km are appropriate for the transfer trajectories constructed here. The final transfer trajectory constructed in this chain of nominal solutions is the transfer path, desired at the outset, that moves a spacecraft between orbits A and B. The determination of a transfer from halo orbit A to each subsequent intermediate halo, and finally to halo orbit B, employs knowledge of the preceding nominal solution to continue or progress the algorithm; consequently, the sequential routine outlined above is an example of a type of *continuation algorithm.*

IV. Optimization of a Nominal Transfer Trajectory.

The construction of a nominal transfer is accomplished without consideration for the magnitude of the impulsive maneuvers necessary to implement the transfer; consequently, the optimality of a reference solution must be examined. Let $\bar{x} = (x, y, z)^T$ and $\bar{v} = (v_x, v_y, v_z)^T$ represent a spacecraft's position and velocity, respectively, expressed in coordinates relative to the libration point and in the usual rotating frame associated with the restricted three-body problem. Then the equations of motion of the spacecraft are written

$$\ddot{\bar{x}} = \begin{Bmatrix} 2nv_y + \dot{n}y + U_x \\ -2nv_x - \dot{n}x + U_y \\ U_z \end{Bmatrix}, \qquad (16)$$

where n is the angular velocity associated with the primary motion and U_x, U_y, U_z are the first partial derivatives of the pseudo-potential U. The position vector must be continuous; however, for impulsive trajectories, the velocity vector will be discontinuous at discrete instances. The optimality criterion is chosen to be the sum of the magnitudes of the velocity increments,

$$J = \sum_k |\Delta\bar{v}_k| .$$

The optimization problem can be stated as follows: Given an initial orbit A and a final orbit B and a nominal transfer between them, determine the transfer trajectory that connects these orbits such that the cost function J is minimized.

Let the adjoint vector to the velocity, which is termed the primer vector, be denoted by $\bar{p}$. Then, the necessary conditions for an optimal time-fixed impulsive transfer trajectory, first developed by Lawden in conjunction with the two-body problem, are reformulated by Hiday and Howell[4] for the elliptic restricted three-body problem (i.e., for a gravitational field that is position-, velocity-, and time-dependent), and can be expressed entirely in terms of the primer vector as:

1. The primer vector satisfies $\ddot{\bar{p}} = G_x\bar{p} + G_v\dot{\bar{p}}$, and it must be continuous with continuous first derivative.
2. The magnitude of the primer vector is less than or equal to one during the transfer with impulses occurring at those instants for which $p = 1$.
3. At an impulse time, the primer vector is a unit vector aligned in the optimal thrust direction.
4. At all interior impulses (not at the initial or final times), $\dot{p} = 0$, and the derivative of the primer vector and the primer itself must be orthogonal (i.e., $\dot{\bar{p}}^T\bar{p} = 0$).

The quantity G_x is a matrix obtained by taking the partial derivative of the right side of (16) with respect to the position variables, and

$$G_v = \begin{bmatrix} 0 & 2n & 0 \\ -2n & 0 & 0 \\ 0 & 0 & 0 \end{bmatrix}.$$

Additionally, the primer vector and the perturbations in the state variables (i.e., $\delta\bar{x}$ and $\delta\bar{v}$) are related by a variational equation,

$$\bar{p}^T\delta\bar{v} - \left(\dot{\bar{p}}^T + \bar{p}^T G_v\right)\delta\bar{x} = \text{constant}, \qquad (17)$$

that is valid between the impulses on a trajectory in the elliptic restricted three-body problem. (In the development of the above conditions, note that significant differences exist between this formulation relative to a time-dependent rotating coordinate frame and the traditional two-body problem.)

If a nominal two-impulse trajectory is non-optimal, then the coincident application of both an initial and a final coast is explored as a means of reducing the total fuel expenditure. This dual coast procedure results in a two-impulse transfer whose terminal points have been moved in time and, consequently, in position. Therefore, execution and optimization of a dual coast transfer yields the optimal time-free two-impulse transfer trajectory between variable endpoints on the given orbits A and B. Let dt_0 and dt_f represent the duration of the coastal arcs in initial orbit A and final orbit B, respectively. Since dt_0 and dt_f can be either positive or negative, the following terminology is employed:

- If $dt_0 > 0$, execute an *initial coast* in A.
- If $dt_0 < 0$, execute an *early departure* from A.
- If $dt_f < 0$, execute a *final coast* in B.
- If $dt_f > 0$, execute a *late arrival* at B.

For a given nominal transfer trajectory, minimum fuel considerations render the optimal choices of sign for the coastal periods.

As determined in Reference 5, the difference in cost between a reference trajectory and a dual coast trajectory is

$$\delta J = -\dot{p}_0\,|\Delta\bar{v}_0|\,dt_0 - \dot{p}_f\,|\Delta\bar{v}_f|\,dt_f\,. \qquad (18)$$

In order for a neighboring dual coast two-impulse trajectory to have a lower cost than the nominal solution, δJ must be made negative; consequently,

$$-\dot{p}_0\,|\Delta\bar{v}_0|\,dt_0 < \dot{p}_f\,|\Delta\bar{v}_f|\,dt_f\,. \qquad (19)$$

Whether criterion (19) is met is dependent upon the sign of the coastal periods and the slope of the primer magnitude at the terminal points of the reference trajectory. If the initial and final slopes of the primer magnitude are zero, the transfer trajectory is optimal. Otherwise, the appropriate choice of coastal arcs that render an improved trajectory is summarized by the following four cases that are representative of all possible combinations of initial and final slope of the primer magnitude:

- If $\dot{p}_0 > 0$ and $\dot{p}_f < 0$, then $dt_0 > 0$ and $dt_f < 0 \rightarrow$ Initial Coast/Final Coast.
- If $\dot{p}_0 > 0$ and $\dot{p}_f > 0$, then $dt_0 > 0$ and $dt_f > 0 \rightarrow$ Initial Coast/Late Arrival.
- If $\dot{p}_0 < 0$ and $\dot{p}_f < 0$, then $dt_0 < 0$ and $dt_f < 0 \rightarrow$ Early Departure/Final Coast.
- If $\dot{p}_0 < 0$ and $\dot{p}_f > 0$, then $dt_0 < 0$ and $dt_f > 0 \rightarrow$ Early Departure/Late Arrival.

The magnitudes of the coastal periods are specified by requiring the largest negative variation in the cost function. Note that equation (18) can be written in the form

$$\delta J = \nabla J \cdot d\bar{z}\,,$$

where $\bar{z}$ is a vector comprised of the times of the initial and final impulsive maneuvers. Thus, the problem of determining an optimal trajectory becomes one of minimizing $J(\bar{z})$ by a multivariable search method. Since the gradients are known analytically in terms of the initial and final impulses and the derivative of the primer vector at the terminal points of the reference trajectory, a minimizing technique that utilizes the gradient components is indicated. One such technique

that has been employed is the Broydon-Fletcher-Goldfarb-Shanno variable metric method for unconstrained minimization which is available in the Automated Design Synthesis (ADS) package developed by Vanderplaats.[8]

Once the coastal periods that minimize the cost function are determined, the time of flight (TOF) on the transfer trajectory is established and subsequently unmodified. The primer magnitude plot of the resultant transfer should display terminal points of zero slope. Additionally, if the primer magnitude, with the exception of the endpoints, lies entirely below unity, this two-impulse time-free transfer is optimal. However, should the primer magnitude exceed unity at any instant, then one or more impulsive maneuvers should be executed interior to the initial and final impulses such that the overall fuel consumption is diminished. Specification of the location, magnitude, and direction of the additional intermediate impulses is achieved utilizing the methodology developed for multi-impulse time-fixed transfers between libration-point orbits.[4]

V. Results

Three cases are investigated for which inferior transfers are constructed from initial halo orbits characterized by z-amplitudes of 160,000 km (Case I1), 200,000 km (Case I2), and 240,000 km (Case I3). A z-amplitude of $A_z = 110{,}000$ km is imposed on the final halo orbit. For each of the inferior transfers, the date of injection into the initial halo orbit is specified as August 17; also, the departure and arrival locations are selected to be the maximum z-excursions on the halo orbits. The initial phase angles are chosen such that the spacecraft is injected near the point of maximum z-excursion on the initial halo orbit. The spacecraft then proceeds for approximately one revolution in a counter-clockwise direction in the y-z projection prior to commencement of the 1-rev transfer segment. Arrival at the final halo orbit occurs near its maximum z-excursion, and the trajectory concludes with one revolution in the final halo. So, each nominal trajectory contains three complete revolutions in the y-z plane. The nominal transfer trajectories for cases I1-I3 are constructed utilizing the spiral method, the differential corrections procedure, and the continuation algorithm outlined above. The z-amplitude increment ΔA_z is chosen to assume the values 10,000 km and 20,000 km for the creation of the nominal transfer in case I1 and the values of 40,000 km and 50,000 km for the creation of the nominal transfers in cases I2 and I3.

Plotted relative to the libration point L_1, the y-z projection of the two-impulse nominal trajectory constructed for case I1 is illustrated in Figure 2. The transfer segment of this trajectory is accomplished in 175.98 days at a cost of 160.60 m/s, and the resulting history of the primer magnitude over this portion of the

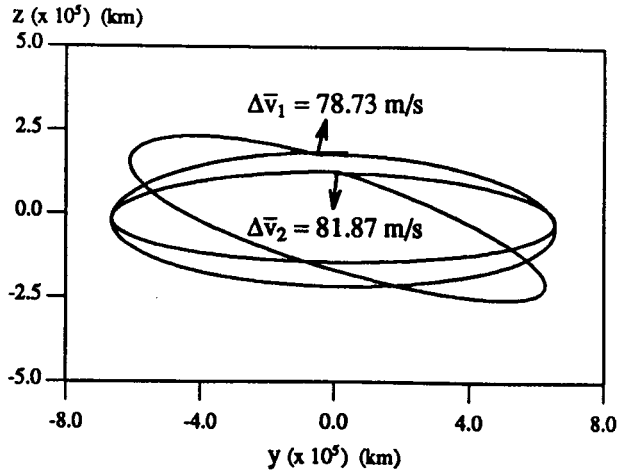

Fig. 2 y-z Projection of 2-Impulse Nominal Trajectory (Case I1); $|\Delta\bar{v}| = 160.60$ m/s; Transfer TOF = 175.98 days

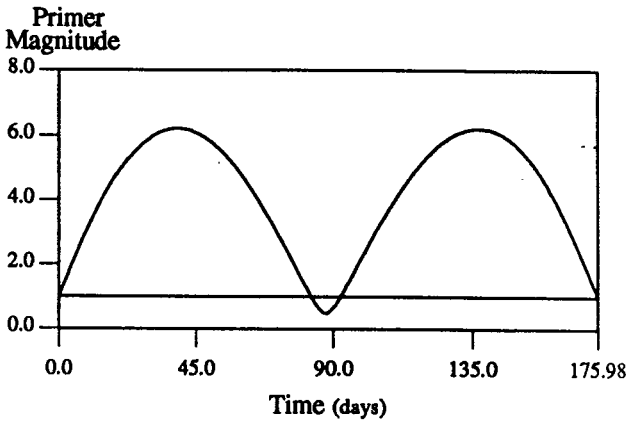

Fig. 3 Primer Magnitude History of 2-Impulse Nominal Transfer (Case I1); $|\Delta\bar{v}| = 160.60$ m/s

trajectory is shown in Figure 3. Clearly, the slopes of the primer magnitude at the initial and final instant are unequal to zero; thus, the cost on the nominal transfer can be improved by the inclusion of coasts on the initial and final halo orbits. Since the slopes of the primer magnitude at the initial and final instants on the reference solution are positive and negative, respectively, an initial coast ($dt_0 > 0$) and a final coast ($dt_f < 0$) are warranted. The optimized coastal periods are determined to be $dt_0 = 22.83$ days and $dt_f = -24.02$ days. In order to illustrate these coastal periods, the corresponding primer magnitude history is plotted relative to the time of flight on the nominal transfer [See Figure 4]. Although the slopes of the primer magnitude at the endpoints of the transfer are zero, the primer magnitude still lies, in part, above unity and indicates that the cost on the resulting trajectory can be improved. Despite being non-optimal, the corresponding trajectory [See Figure 5], which is executed at a cost of only 28.16 m/s (a substantial saving of 132.44 m/s over the nominal solution) and which is accomplished in 129.13 days,

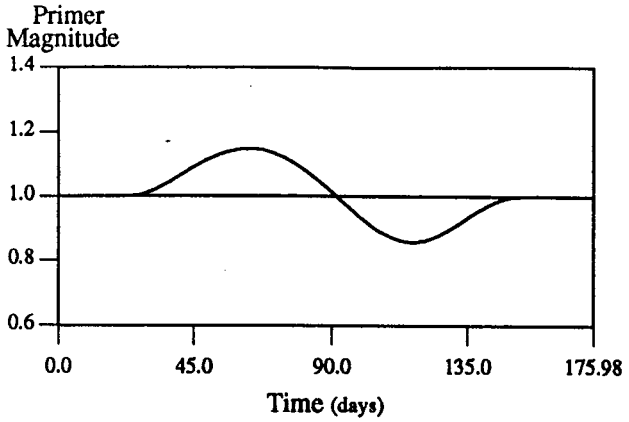

Fig. 4 Primer Magnitude History of Best 2-Impulse Transfer (Case I1); $|\Delta\bar{v}| = 28.16$ m/s

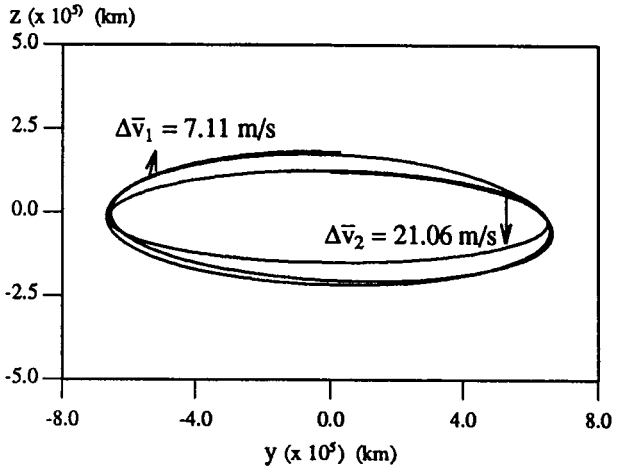

Fig. 5 y-z Projection of Best 2-Impulse Transfer (Case I1); $|\Delta\bar{v}| = 28.16$ m/s; Transfer TOF = 129.13 days

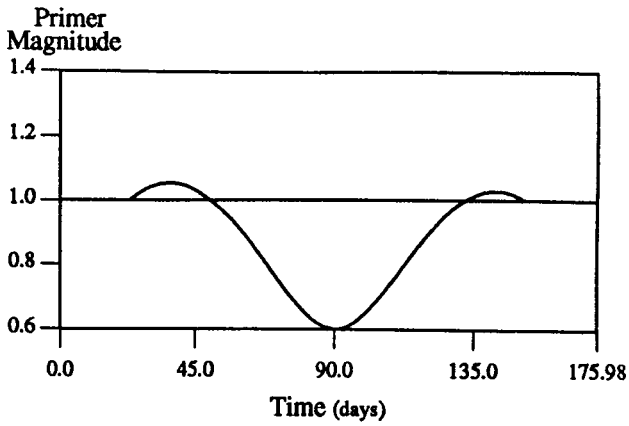

Fig. 6 Primer Magnitude History of Best 3-Impulse Transfer (Case I1); $|\Delta\bar{v}| = 26.38$ m/s

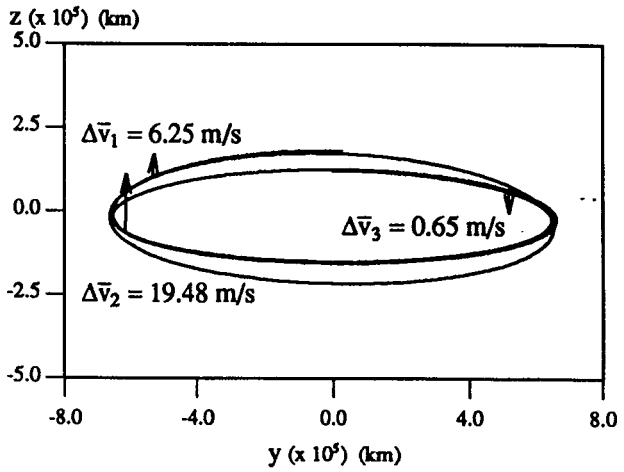

Fig. 7 y-z Projection of Best 3-Impulse Transfer (Case I1); $|\Delta\bar{v}| = 26.38$ m/s; Transfer TOF = 129.13 days

represents the *best* time-free two-impulse transfer trajectory obtained for case I1. Examination of Figure 5 shows that the coastal arcs drive the departure and arrival locations on the halo orbits toward points of minimum and maximum y-excursion, respectively.

A further reduction in cost can only be achieved by the addition of interior impulses. One, two, and three interior impulses are applied, and the locations and times of each impulse are optimized prior to the application of the next impulse; however, an optimal solution is elusive. Illustrated in Figures 6 and 7 are the primer magnitude history and the y-z projection of the best complete trajectory that contains one interior impulse. Notice that application of an interior impulse results in non-zero slopes at the endpoints of the primer magnitude history plotted in Figure 6. Restoration of these slopes to zero would require the simultaneous optimization of the coastal periods and the timing and location of the interior impulse, but such an approach destroys the integrity of the numerical solutions for the initial and final halo orbits. Thus, the coastal periods are unaltered during the optimization of the interior impulse. The time-free three-impulse transfer illustrated in Figure 7 is accomplished at a cost of 26.38 m/s, and only minuscule reductions in cost are achieved by the application of the subsequent interior impulses. The difficulty in obtaining an *optimal* solution results in part from omission of coastal period modification during interior impulse application and the ensuing optimization. Representing a compromise between a practical number of impulsive maneuvers and the greatest reduction in fuel expenditure, the three-impulse trajectory of Figure 7 is considered to be the *best* time-free transfer trajectory for case I1 that results from this procedure.

The two-impulse nominal solutions are constructed for cases I2 and I3, and the corresponding primer magnitude histories are very similar to that of case I1 [See Figure 3]. The time-free optimizations of cases I2 and I3 follow the trends established by case I1. Figures 8-9 (case I2) and 12-13 (case I3) illustrate the plots of the primer magnitude over the duration of the best time-

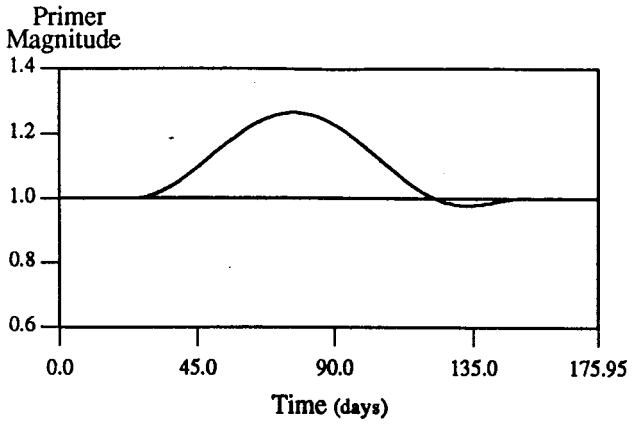

Fig. 8 Primer Magnitude History of Best 2-Impulse Transfer (Case I2); $|\Delta\bar{v}|$ = 44.26 m/s

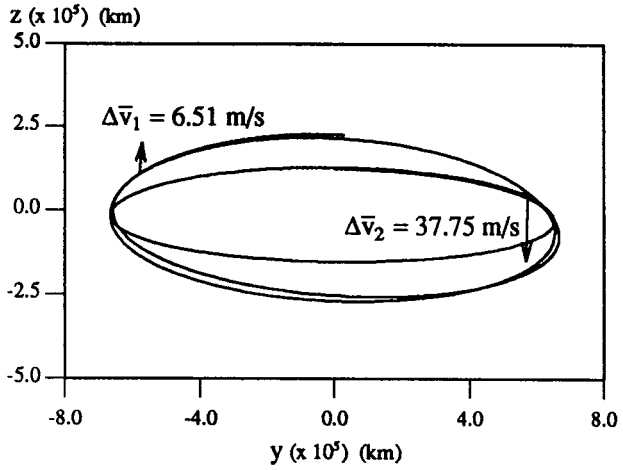

Fig. 9 y-z Projection of Best 2-Impulse Transfer (Case I2); $|\Delta\bar{v}|$ = 44.26 m/s; Transfer TOF = 122.61 days

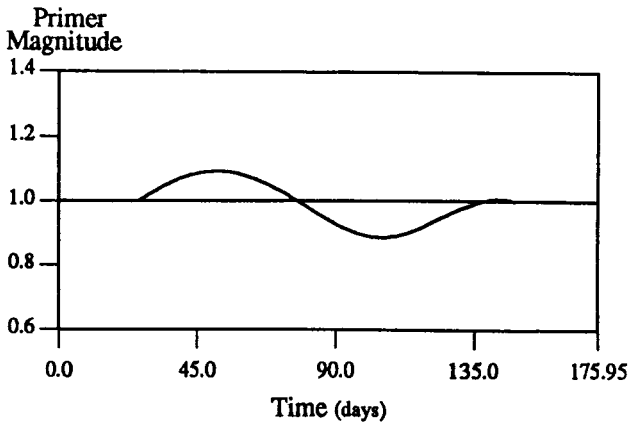

Fig. 10 Primer Magnitude History of Best 3-Impulse Transfer (Case I2); $|\Delta\bar{v}|$ = 44.20 m/s

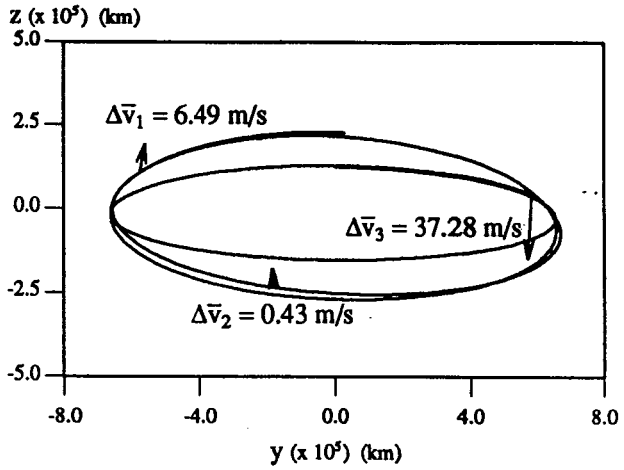

Fig. 11 y-z Projection of Best 3-Impulse Transfer (Case I2); $|\Delta\bar{v}|$ = 44.20 m/s; Transfer TOF = 122.61 days

free two-impulse transfers and the y-z projections of the corresponding trajectories. Once again, the coastal periods act to move the departure and arrival locations toward the extreme y-excursions. Also, the cost on the time-free two-impulse trajectory is reduced substantially from 254.95 m/s to 44.25 m/s in case I2 and from 339.64 m/s to 65.03 m/s in case I3. Interior impulses are applied in an effort to further reduce the cost necessary to implement each transfer. The resulting best three-impulse primer magnitude histories and corresponding y-z projections are displayed in Figures 10-11 and Figures 14-15 for cases I2 and I3, respectively. Supplementary interior impulses produce little reduction in cost; thus, the time-free three-impulse transfer trajectories of Figures 11 (case I2) and 15 (case I3) are again deemed the best compromise between fuel economy and practicality of maneuver occurrences.

In each of the three cases investigated, the best time-free two-impulse transfer trajectory [See Figures 5, 9, and 13] has a duration of approximately three-quarters of a revolution using a fairly small initial impulsive maneuver followed by a final maneuver of significant magnitude. The primer magnitude histories [See Figures 4, 8, and 12] for these two-impulse solutions are all very similar. After the application and optimization of an interior impulse, however, the distribution of $|\Delta\bar{v}|$ expenditure is altered. For case I1, the interior impulse applied near the minimum y-excursion becomes the dominant impulsive maneuver; whereas, for cases I2 and I3, the magnitude of the interior impulse is quite small, and the final maneuver retains its strength.

Table 1 summarizes the fuel expenditures on the inferior transfers for cases I1-I3. Although *optimal* solutions are not obtained in any of the three cases examined, the inferior transfers resulting from the time-free optimization process do exhibit a dramatic decrease in fuel expenditure compared to the nominal two-impulse solutions; moreover, the cost on the best three-impulse transfer trajectory varies nearly linearly with increasing z-amplitude of the initial halo orbit. Additionally, the application of coastal arcs in the initial

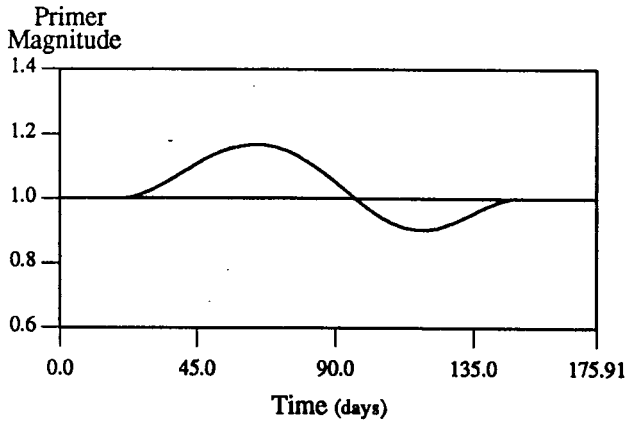

Fig. 12 Primer Magnitude History of Best 2-Impulse Transfer (Case I3); $|\Delta\bar{v}|$ = 65.03 m/s

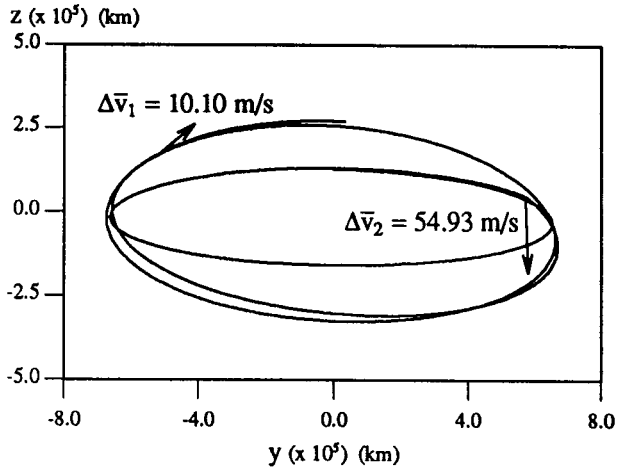

Fig. 13 y-z Projection of Best 2-Impulse Transfer (Case I3); $|\Delta\bar{v}|$ = 65.03 m/s; Transfer TOF = 127.22 days

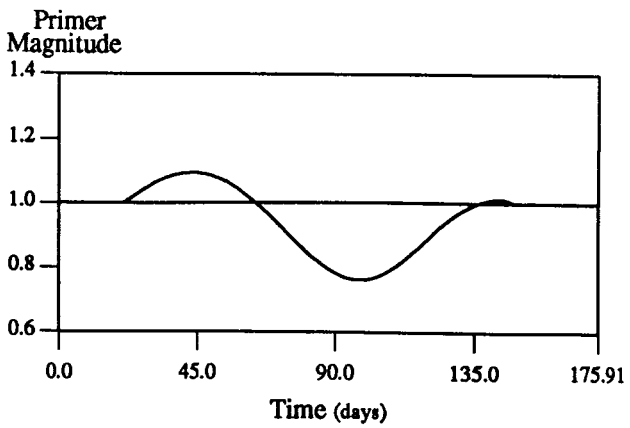

Fig. 14 Primer Magnitude History of Best 3-Impulse Transfer (Case I3); $|\Delta\bar{v}|$ = 65.90 m/s

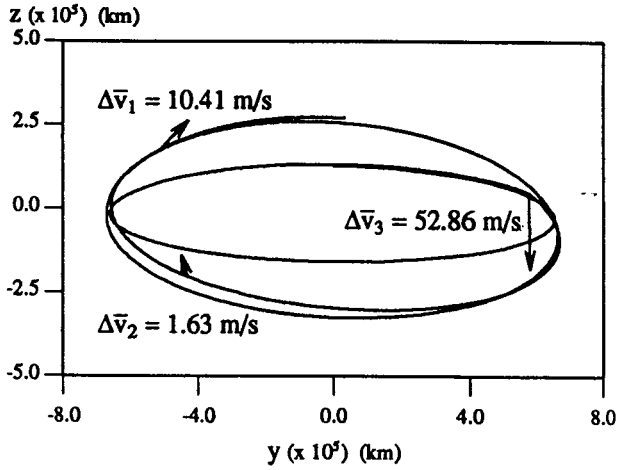

Fig. 15 y-z Projection of Best 3-Impulse Transfer (Case I3); $|\Delta\bar{v}|$ = 64.90 m/s; Transfer TOF = 127.22 days

and final halo orbits tends to drive the departure and arrival locations toward the extreme y-excursions in each case; however, no clear relationship appears to exist between the time of flight on the transfer and the z-amplitude of the initial orbit.

In order to investigate the effect of declivity and acclivity on the cost of a transfer trajectory between two libration-point orbits, the correlation is explored between the superior time-free transfers S1-S3, constructed in Reference 5 and summarized in Table 1, and the inferior transfers presented above. Transfers between halo orbits of equal z-amplitude gradations are examined; therefore, compare cases S1 and I1, cases S2 and I2, and cases S3 and I3. The inferior nominal transfers are accomplished using substantially less fuel than that required on analogous superior nominal transfers; however, the best inferior trajectories require greater $|\Delta\bar{v}|$ expenditures than do the optimized superior trajectories in order to implement a transfer between halo orbits of similar separation. The fuel expenditures associated with cases S1 and I1 are roughly equal, but the solutions are quite different. Whereas an optimal solution in case S1 is attained with only two impulses and supplementary interior impulses are not necessary for cost reduction, even a five-impulse solution in case I1 is non-optimal. However, the best three-impulse transfer for case I1 is comparable in fuel expenditure and time of flight to the optimal two-impulse transfer trajectory for case S1. For the two remaining pairs of cases, optimal solutions are not rendered; thus, the best three-impulse trajectories are compared. The cost on both of the inferior transfers in cases I2 and I3 exceed the cost on the superior transfers constructed in cases S2 and S3, and this cost discrepancy appears to increase with separation between initial and final orbits. Additionally, the decrease in time of flight with increased z-amplitude separation that is characteristic of the superior transfers is not representative of the inferior transfers, for no distinct trend in time-of-flight variation is established in cases I1-I3. These observations suggest further development of a method to simultaneously modify the coastal periods and the characteristics of the

Table 1 Costs on Inferior and Superior Transfers between Halo Orbits

Case	Z-Amplitude of Initial Halo (km)	Z-Amplitude of Final Halo (km)	Nominal 2-Impulse Transfer $\lvert\Delta\bar{v}\rvert$ (m/s)	Nominal 2-Impulse Transfer TOF (days)	Improved Time-Free Transfers 2-Impulse $\lvert\Delta\bar{v}\rvert$ (m/s)	Improved Time-Free Transfers 3-Impulse $\lvert\Delta\bar{v}\rvert$ (m/s)	Improved Time-Free Transfers TOF (days)
I1	160,000	110,000	160.60	175.98	28.16	26.38	129.13
I2	200,000	110,000	254.95	175.95	44.26	44.20	122.61
I3	240,000	110,000	339.64	175.91	65.03	64.90	127.22
S1	110,000	160,000	198.46	175.98	26.96†	NA	132.72
S2	110,000	200,000	386.59	177.20	37.65	37.59	116.86
S3	110,000	240,000	447.32	177.20	49.08	49.06	108.95

† Resultant trajectory is optimal.

interior impulse such that the initial and final path constraints (to match the halo orbits) are satisfied. An investigation of this issue is underway.

VI. Summary

This study involves the successful development of a methodology for the optimization of time-free inferior impulsive transfer trajectories between variable endpoints on halo orbits in the vicinity of the interior L_1 libration point of the Sun-Earth/Moon barycenter system. The strategy outlined above is enabled by the construction of a nominal transfer using a differential corrections routine and a continuation algorithm. The subsequent application of primer vector theory to this non-optimal reference trajectory determines whether the implementation of coasts on the initial and final orbits reduces fuel expenditure. Although *optimal* solutions are not obtained, results indicate that a substantial savings in fuel expenditure can be achieved by the allowance for coastal periods on the halo orbits; also, the presence of coastal arcs drives the departure and arrival location toward the extreme y-excursions of the halo orbits. Finally, initial results include costs necessary to implement inferior transfers that are greater than those required on superior transfers between halo orbits of equal z-amplitude separation. Examination of these results is continuing.

VII. References

1. Lawden, D. F., *Optimal Trajectories for Space Navigation*, Butterworths, London, 1963.
2. Pernicka, H. J., "The Numerical Determination of Nominal Libration Point Trajectories and Development of a Station-Keeping Strategy," Ph.D. Dissertation, School of Aeronautics and Astronautics, Purdue University, May 1990.
3. Gómez, G., Jorba, A., Masdemont, J., and Simó, C., "Study Refinement of Semi-Analytical Halo Orbit Theory," European Space Agency Contract No. 8625/89/D/MD(SC), Final Report, April 1991.
4. Hiday, L. A. and Howell, K. C., "Transfers Between Libration-Point Orbits in the Elliptic Restricted Problem," AAS/AIAA Space Flight Mechanics Conference, AAS-92-126, Colorado Springs, CO, February 24-26, 1992.
5. Hiday, L. A. and Howell, K. C., "Impulsive Time-Free Transfers Between Halo Orbits," AIAA/AAS Astrodynamics Conference, Hilton Head, SC, August 10-12, 1992.
6. Richardson, D. L., "Analytic Construction of Periodic Orbits About the Collinear Points," *Celestial Mechanics*, Vol. 22, 1980, pp. 241-253.
7. Howell, K. C. and Pernicka, H. J., "Numerical Determination of Lissajous Trajectories in the Restricted Three-Body Problem," *Celestial Mechanics*, Vol. 41, 1988, pp. 107-124.
8. Vanderplaats, G. N., *ADS—A Fortran Program for Automated Design Synthesis*, Version 1.10, May 1985.